Secondary instabilities of linearly heated falling films*

HU Jun[1]**, SUN Dejun[1], HU Guohui[2] and YIN Xieyuan[1]

(1. Department of Modern Mechanics, University of Science and Technology of China, Hefei 230027, China; 2. Institute of Applied Mathematics and Mechanics, Shanghai University, Shanghai 200072, China)

Received May 9, 2004; revised September 28, 2004

Abstract Secondary instabilities of linearly heated falling films are studied through three steps. Firstly, the analysis of the primary linear instability on Miladinova's long wave equation of the linearly heated film is performed. Secondly, the similar Landau equation is derived through weak nonlinear theory, and a two-dimensional nonlinear saturation solution of primary instability is obtained within the weak nonlinear domain. Thirdly, the secondary (three-dimensional) instability of the two-dimensional wave is studied by the Floquet theorem. Our secondary instability analysis shows that the Marangoni number has destabilization effect on the secondary instability.

Keywords: linearly heated falling film, secondary instability, Floquet theorem.

Since Kapitza experimentally studied the film flow on an inclined plane[1,2], the mechanics of film instability has been extensively studied theoretically, from linearity to nolinearity, and from isothermal to heated film. By linear instability analysis, the surface and shear modes have been identified for isothermal films, though the surface mode is dominant when the inclined angle is not very small. However, for uniformly heated film, there exists another two types of thermocapillary instability. As for nonlinear instability, weakly nonlinear analysis has shown that there exist supercritical and subcritical instabilities below a cutoff wavenumber. Detailed discussions can be found in the review papers by Chang[3] and Oron et al.[4], and also references therein.

Recently, more and more studies are concerned with falling films on a non-uniformly heated plate. Kalitzova et al.[5] first analysed the linear long-wave instability of thin liquid layer on a linearly heated plate. They investigated the Marangoni effect on the magnitude of the critical Reynolds number. Miladinova et al.[6] extended the problem to the finite-amplitude long-wave instabilities of two-dimensional films. They derived a long-wave nonlinear evolution equation based on the Benney's approach[7] and confirmed the existence of permanent finite-amplitude waves of different kinds. Their linear stability analysis on the evolution equation also shows that the temperature decrease along the plate can stabilize the film flow.

Joo and Davis[8] reported a secondary instability analysis on the isothermal falling films in 1992. They examined the spatially synchronous instability in three steps: (i) primary linear instability on the undisturbed surface; (ii) nonlinear equilibration of primary instability into two-dimensional finite-amplitude permanent wave; (iii) secondary (three-dimensional) instability of the two-dimensional wave. In this paper, we will extend Miladinova's long-wave equation to the secondary instabilities of the linearly heated films in the same three steps.

1 Primary instability and nonlinear saturation

A thin liquid layer falling down from a vertical linearly heated plate is schematically shown in Fig. 1. The film has a mean thickness d, and is bounded by a motionless passive gas with the ambient temperature T_g and pressure p_g. The free surface is assumed adiabatic. The liquid is Newtonian with constant density ρ, kinematic viscosity ν and thermal diffusivity κ. The surface tension σ depends linearly on the temperature T:

$$\sigma = \sigma_0 - \gamma(T - T_g), \tag{1}$$

where σ_0 is the mean surface tension at temperature T_g, and $\gamma = -d\sigma/dT$ is a positive constant for most common liquids. The origin is located on the plate surface, where the temperature is equal to T_g. The wall temperature T_w is given by

* Supported by National Natural Science Foundation of China (Grant No. 10002018) and the Chinese Academy of Sciences (Grant No. KJCX2-SW-L2)

** To whom correspondence should be addressed. E-mail: hucom@mail.ustc.edu.cn

?1994-2018 China Academic Journal Electronic Publishing House. All rights reserved. http://www.cnki.net

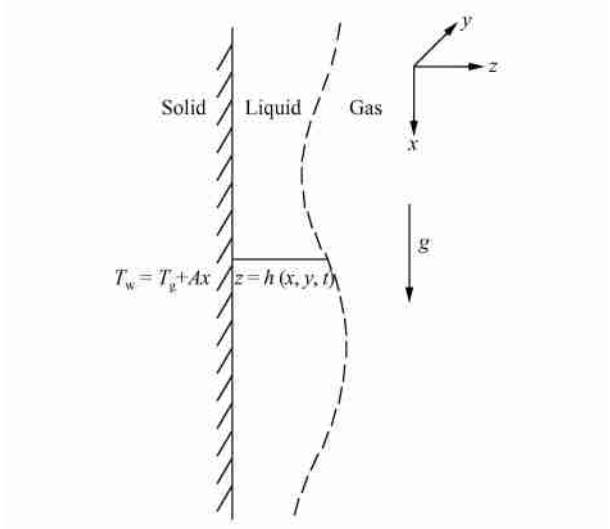

Fig. 1. Schematic diagram of a linearly heated vertically falling film.

$$T_w = T_g + Ax, \tag{2}$$

and it increases (decreases) in the streamwise direction with a positive (negative) constant gradient A. The characteristic length l in the streamwise or spanwise direction (proportional to a typical wavelength of the interface) is much larger than d. Miladinova et al.[6] have shown that using the Benney's long-wave theory the local film thickness $h(x, y, t)$ can be represented as a nonlinear evolution equation:

$$h_t + (Gh - Mn)hh_x + \varepsilon\left[\frac{2}{15}Gh^5 h_x(Gh - Mn)\right]_x + \varepsilon\nabla\cdot\left[\frac{1}{2}Pr\cdot Mn\cdot h^4\left(\frac{5}{6}Gh - Mn\right)\nabla h + Sh^3\nabla\nabla^2 h\right] + O(\varepsilon^2) = 0, \tag{3}$$

where x and y, scaled by l, are streamwise and spanwise coordinates, h and t are scaled by d and ld/ν, respectively. ∇ is a 2D gradient operator (∂_x, ∂_y), $\varepsilon = d/l \ll 1$. In Eq. (3), G is the Reynolds number,

$$G = \frac{gd^3}{\nu^2}, \tag{4}$$

where g is the gravitational acceleration. The surface tension σ is measured by

$$S = \varepsilon^2\frac{\rho\sigma_0 d}{3\mu^2}, \quad \text{or} \quad F = SG^{-\frac{1}{3}}, \tag{5}$$

where $\mu = \rho\nu$ is the dynamic viscosity, F is independent of the mean thickness d; and Mn is represented by

$$Mn = \frac{Ma}{Pr}, \tag{6}$$

where Ma and Pr are the Marangoni number and the Prandtl number, respectively, defined by

$$Ma = \frac{\gamma A d^2}{\mu\kappa}, \quad Pr = \frac{\nu}{\kappa}. \tag{7}$$

As described by Joo and Davis[8], the second term in Eq. (3) is nonlinear, which describes the propagation, and local steepening of disturbance waves. The third term in Eq. (3) describes the mean flow, and is responsible for the surface wave instability. The fourth term (or the first term in the last square bracket) in Eq. (3) describes the Marangoni effects on the surface wave instability. The last term describes the stabilizing capillary effects.

The basic state for the primary instability is a uniform undisturbed one. We impose an infinitesimal harmonic disturbance

$$h(x, y, t) = 1 + \delta_0\exp[\mathrm{i}(\boldsymbol{k}\cdot\boldsymbol{r} - \omega t)], \tag{8}$$

where the disturbed amplitude $\delta_0 \ll 1$, and the wavenumber vector $\boldsymbol{k} = (k\cos\varphi, k\sin\varphi)$, φ is the angle of the oblique wave propagating in the (x, y)-plane. Substituting Eq. (8) into the evolution equation Eq. (3), we can obtain the linearized phase speed c_L, and the linear growth rate ω_i, the imaginary part of ω,

$$c_L = G - Mn, \tag{9}$$

$$\omega_i = \varepsilon k^2\left[\frac{2}{15}G(G - Mn)\cos^2\varphi - k^2 S + \frac{5}{12}G\cdot MnPr - \frac{1}{2}PrMn^2\right]. \tag{10}$$

Roskes[9] pointed out that for the case of $Mn = 0$, namely, for isothermal films, the three-dimensional oblique wave can be reduced into a two-dimensional one by a simple coordinate rotation (replace $G\cos\varphi$ by G, and set $\partial_y = 0$). However, it is impossible for the case of $Mn \neq 0$. In the following discussion, we only study the situation of $\varphi = 0$. According to Eq. (10), we can obtain the critical Reynolds number G_c and the critical wavenumber k_c,

$$G_c = a + \sqrt{a^2 + b}, \tag{11}$$

$$k_c = \sqrt{\frac{D}{S}}, \tag{12}$$

where

$$a = -\frac{25}{16}\left(Pr - \frac{8}{25}\right)Mn, \quad b = \frac{15}{4}PrMn^2, \tag{13}$$

$$D = \frac{2}{15}G(G - Mn) + \frac{5}{12}G\cdot MnPr - \frac{1}{2}PrMn^2. \tag{14}$$

And the maximum linear growth rate occurs at $k = k_m = k_c/\sqrt{2}$.

?1994-2018 China Academic Journal Electronic Publishing House. All rights reserved. http://www.cnki.net

For isothermal film flow, the weakly nonlinear analysis predicts that the evolution of the two-dimensional waves depends strongly on the initial wavenumber k[10—12]. There exists a value of k_{su}, the flow is supercritically stable and nonlinear saturation occurs after the initial linear instability when $k_{su}<k<k_c$; and the nonlinearity, on the other hand, promotes the instability and the saturation does not occur when $0<k<k_{su}$ (subcritical bifurcation). In the supercritical region, for a wavenumber k close to k_c, the solution evolves into a stable, almost sinusoidal wave of small finite amplitude, and for k close to k_m, the surface wave approaches the form of a solitary wave, as observed in experiments. These conclusions above have been verified by numerical simulations based on the Benney's long-wave approximation[13]. In this section, the same weakly nonlinear analysis as Gjevik's[8] will be extended to non-isothermal film.

Applying the weakly nonlinear theory, the free surface evolution can be well approximated by the fundamental wave and its few lowest harmonics

$$h(x,t)=1+\sum_{n=1}^{N}A_n(t)e^{iknx}+c.c., \quad (15)$$

where $c.c.$ denotes complex conjugate. Substituting Eq. (15) into Eq. (3) by setting $N=2$, we obtain a minimal representation

$$\dot{A}_1=\alpha_1A_1+\beta_1A_1^*A_2+\gamma_1|A_1|^2A_1+2\gamma_1|A_2|^2A_1, \quad (16)$$

$$\dot{A}_2=\alpha_2A_2+\beta_2A_1^2+2\gamma_2|A_1|^2A_2+\gamma_2|A_2|^2A_2, \quad (17)$$

where the dot denotes derivative with respect to time, superscript * denotes complex conjugate and the coefficients α_i, β_i and γ_i ($i=1,2$) are listed in the Appendix. We assume that $|A_n|\sim O(\varepsilon^n)$ and $\varepsilon\ll1$, thus

$$\dot{A}_1=\alpha_1A_1+\beta_1A_1^*A_2+\gamma_1|A_1|^2A_1+O(\varepsilon^5), \quad (18)$$

$$\dot{A}_1=\alpha_2A_2+\beta_2A_1^2+O(\varepsilon^4). \quad (19)$$

It is convenient to set $A_1=B_1\exp(i\theta_1)$, $A_2=B_2\exp(i\theta_2)$, and $\phi=\theta_2-2\theta_1$, where B_i, θ_i ($i=1,2$) and ϕ are real functions of time. Then Eqs. (18) and (19) can be reduced into a system of real nonlinear differential equations

$$\dot{B}_1=\alpha_{1r}B_1+[\beta_{1r}\cos\phi-\beta_{1i}\sin\phi]B_1B_2+\gamma_{1r}B_1^3+O(\varepsilon^5), \quad (20)$$

$$\dot{B}_2=\alpha_{2r}B_2+[\beta_{2r}\cos\phi+\beta_{2i}\sin\phi]B_1^2+O(\varepsilon^4), \quad (21)$$

$$\dot{\phi}=[\beta_{2i}\cos\phi-\beta_{2r}\sin\phi]B_1^2/B_2+O(\varepsilon^2), \quad (22)$$

where subscripts r and i denote the real and imaginary parts, respectively. There exists a non-trivial steady solution by setting $\dot{B}_1=\dot{B}_2=\dot{\phi}=0$, which is as follows:

$$B_1=\left(\frac{\alpha_{1r}\alpha_{2r}}{\beta_{1r}\beta_{2r}-\beta_{1i}\beta_{2i}-\gamma_{1r}\alpha_{2r}}\right)^{\frac{1}{2}}, \quad (23)$$

$$B_2=\frac{\alpha_{1r}(\beta_{2r}^2+\beta_{2i}^2)^{\frac{1}{2}}}{\beta_{1r}\beta_{2r}-\beta_{1i}\beta_{2i}-\gamma_{1r}\alpha_{2r}}, \quad (24)$$

$$\phi=\pi+\arctan(\beta_{2i}/\beta_{2r}), \quad (25)$$

where ϕ lies in the second quadrant. From Eq. (23), we can obtain the existing condition

$$\frac{\alpha_{1r}\alpha_{2r}}{\beta_{1r}\beta_{2r}-\beta_{1i}\beta_{2i}-\gamma_{1r}\alpha_{2r}}>0. \quad (26)$$

Because $|\beta_{1i}\beta_{2i}|\gg|\beta_{1r}\beta_{2r}|$, $|\beta_{1i}\beta_{2i}|\gg|\gamma_{1r}\alpha_{2r}|$, and $\beta_{1i}\beta_{2i}>0$, thus $\alpha_{1r}\alpha_{2r}<0$, i.e.

$$\left[\frac{2}{15}G^2-\frac{2}{15}GMn\left(1-\frac{25}{8}Pr\right)-\frac{1}{2}PrMn^2-k^2S\right]\times\left[\frac{8}{15}G^2-\frac{8}{15}GMn\left(1-\frac{25}{8}Pr\right)-2PrMn^2-16k^2S\right]<0, \quad (27)$$

which can result in $k_{su}<k<k_c$, and $k_{su}=k_c/2$. In a reference frame x' moving with a nonlinear phase velocity c, the flow is steady and the free surface can be expressed as

$$h(x')=1+2[B_1\cos(kx')+B_2\cos(2kx'+\phi)], \quad (28)$$

$$-kc=\dot{\theta}_1=\alpha_{1i}+(\beta_{1r}\sin\phi+\beta_{1i}\cos\phi)B_2+\gamma_{1i}B_1^2+O(\varepsilon^4). \quad (29)$$

Figs. 2 and 3 show features of the saturated nonlinear 2D-permanent wave from Eqs. (23)—(25) with different Mn values when $G=5$, $F=1$, $\varepsilon=0.1$, and $Pr=10$. From Fig. 2 we can see that with the increasing of Mn, the maximum amplitudes $|A_n|$ of the permanent wave become larger for $k_{su}<k<k_c$. The amplitude $|A_1|$ of the fundamental mode increases rapidly and reaches a maximum before k reaches k_m (Fig. 2(a)), and the magnitude $|A_2|$ of the harmonic mode increases monotonically and becomes dominant near $k=k_{su}$ (Fig. 2(b)) as k decreases from k_c. In our weakly nonlinear analysis, we assume that $|A_2|\ll|A_1|$, and therefore the permanent wave in Eq. (28) is only valid in that case. We can easily see from Fig. 2 that the condition is not satisfied near $k=k_{su}$. In Fig. 3, the nonlinear phase velocity is plotted and the results at $k=k_c$ are equal to $G-Mn$, which satisfies the linear analysis. Near $k=k_c$ the phase speed decreases with the decreasing

?1994-2018 China Academic Journal Electronic Publishing House. All rights reserved. http://www.cnki.net

of k, and reaches a minimum, after which it increases and reaches a maximum near k_{su}. For isothermal film flow, our results are the same as that of Joo and Davis[8].

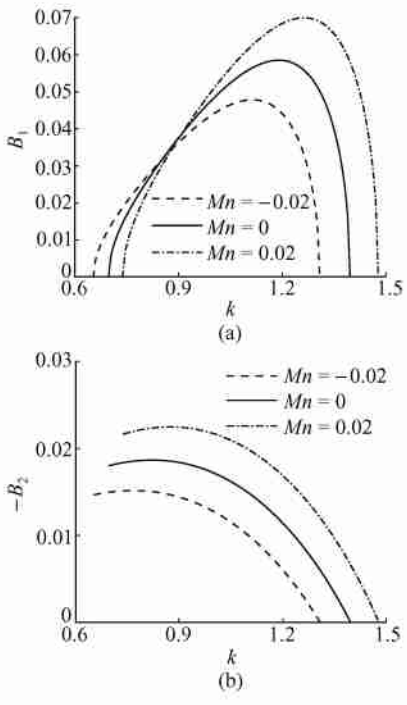

Fig. 2. Magnitudes of (a) mode A_1 and (b) mode A_2 versus the wavenumber k with different Mn values. $G=5$, $F=1$, $\varepsilon=0.1$, $Pr=10$.

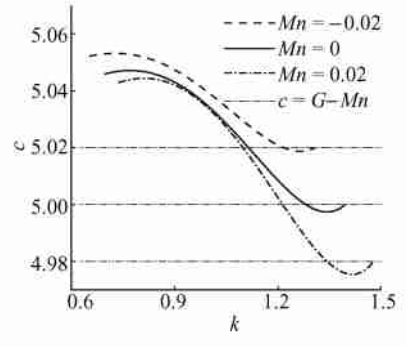

Fig. 3. Nonlinear phase speed c versus the wavenumber k with different Mn values. $G=5$, $F=1$, $\varepsilon=0.1$, $Pr=10$.

If we release the condition $|A_2| \ll |A_1|$ to $|A_2| \sim |A_1|$, but the higher order $|A_n|$ is still very small, then Eqs. (20)—(22) can be changed to

$$\dot{B}_1 = \alpha_{1r}B_1 + [\beta_{1r}\cos\phi - \beta_{1i}\sin\phi]B_1B_2 + \gamma_{1r}B_1^3 + 2\gamma_{1r}B_1B_2^2, \tag{30}$$

$$\dot{B}_2 = \alpha_{2r}B_2 + [\beta_{2r}\cos\phi + \beta_{2i}\sin\phi]B_1^2 + 2\gamma_{2r}B_1^2B_2 + \gamma_{2r}B_2^3, \tag{31}$$

$$\dot{\phi} = [\beta_{2i}\cos\phi - \beta_{2r}\sin\phi]B_1^2/B_2 - 2[\beta_{1i}\cos\phi + \beta_{1r}\sin\phi]B_2 + 2(\gamma_{2i} - \gamma_{1i})B_1^2 + (\gamma_{2i} - 4\gamma_{1i})B_2^2. \tag{32}$$

The non-trivial solution of Eqs. (30)—(32) can be easily obtained using Runge-Kutta method. Fig. 4 shows that the final solutions converge to the steady ones for $k=1.0$, 1.2, when two different initial values of $B_1=0.025$, 0.05, $B_2=-0.0001$, $\phi=0$. These results are compared with those calculated from Eqs. (20)—(22) (Fig. 2), and the relative error is within 1.5%. It should be pointed out that when k

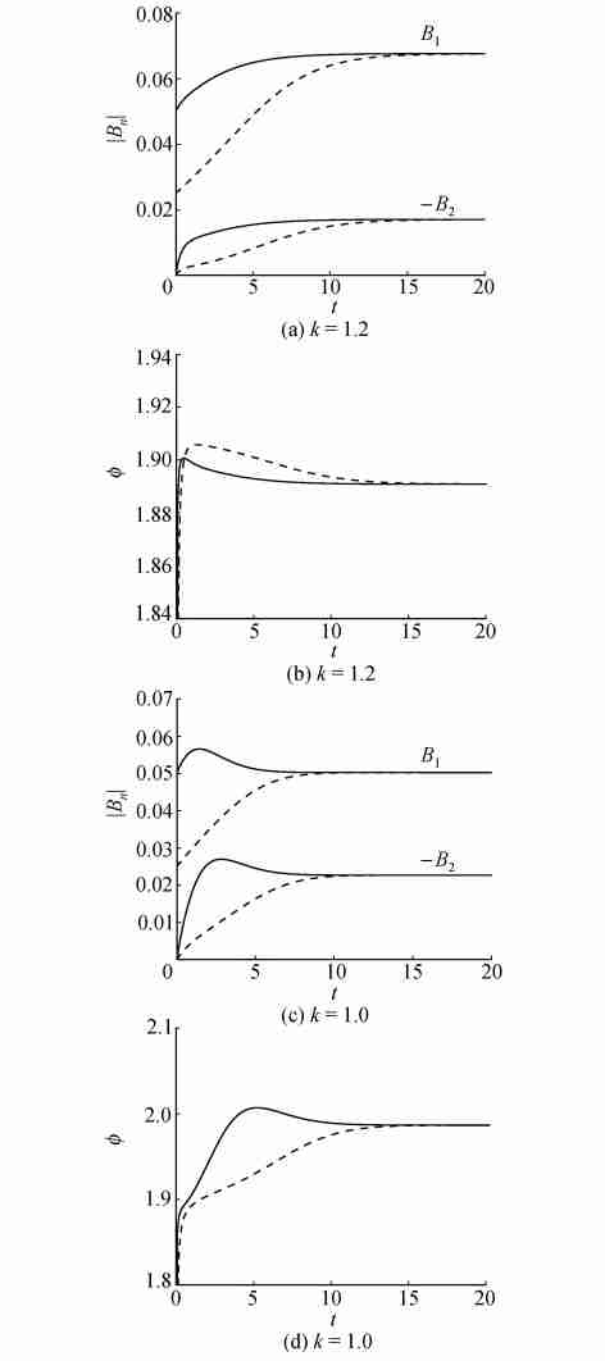

Fig. 4. The nonlinear saturation of the fundamental wave and secondary harmonic with different wavenumbers. $Mn=0.02$, $G=5$, $F=1$, $\varepsilon=0.1$, $Pr=10$.

?1994-2018 China Academic Journal Electronic Publishing House. All rights reserved. http://www.cnki.net

decreases near k_{su}, such as $k=0.8$, the steady solution dose not exist.

Another way to obtain the finite-amplitude permanent wave and confirm the nonlinear saturation is to pose an initial-value problem in a periodic domain and integrate the evolution equation (3) numerically. Miladinova et al.[6] have performed a lot of calculations with different values of k and Mn on an inclined plate (the inclined angle is $\pi/4$). Similar numerical simulations, as shown in Figs. 5 and 6, of the finite-amplitude permanent wave on the vertical plate are carried out using the Runge-Kutta-Verner fifth-order and sixth-order method for the time integration, and using the Fourier-spectral method for the spatial discretization[14].

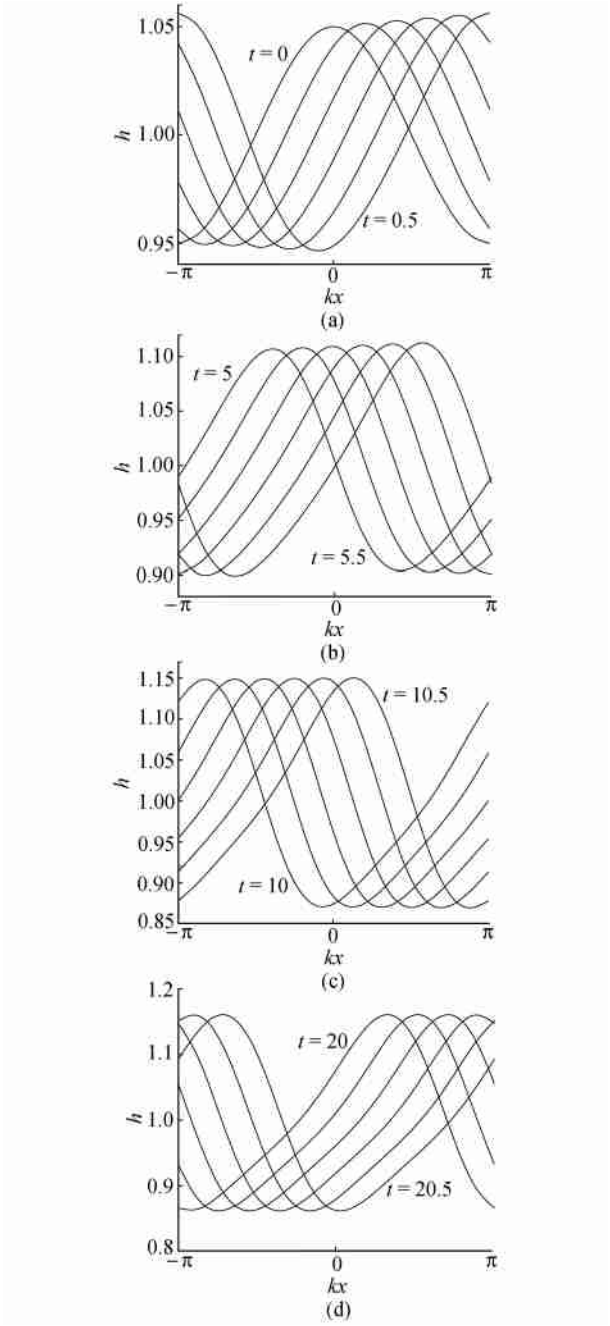

Fig. 5. The nonlinear saturation by numerical computation to the long wave equation with wavenumber $k=1.2$. $Mn=0.02$, $G=5$, $F=1$, $\varepsilon=0.1$, $Pr=10$.

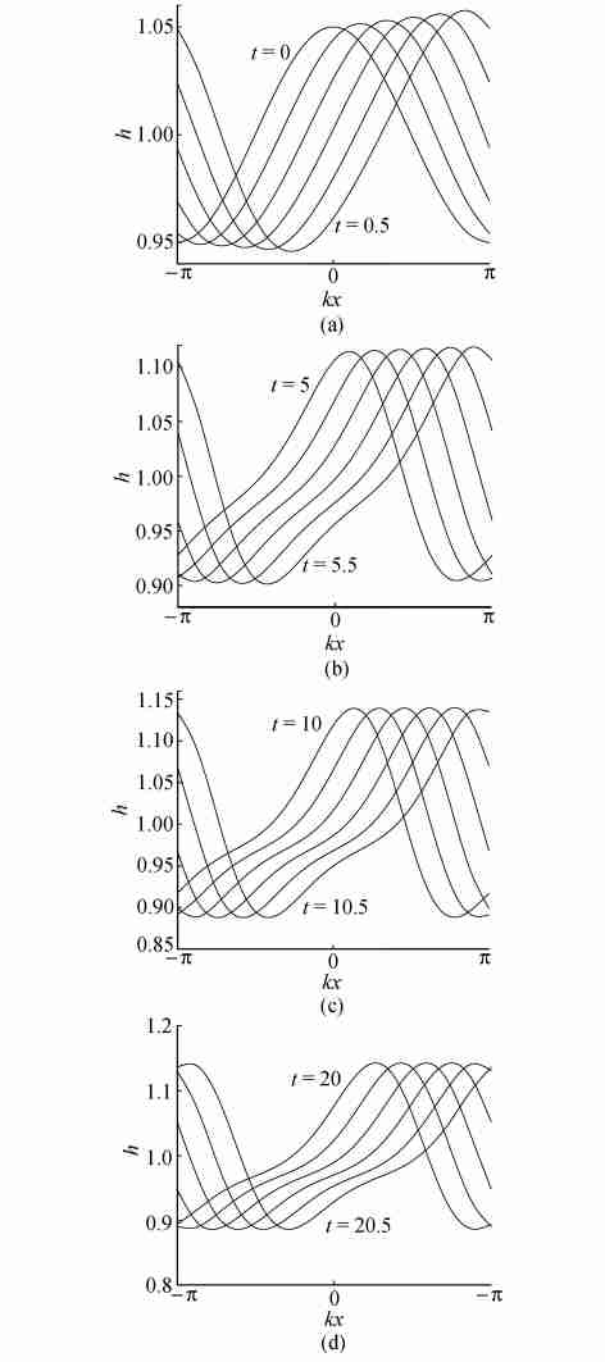

Fig. 6. The nonlinear saturation by numerical computation to the long wave equation with wavenumber $k=1.0$. $Mn=0.02$, $G=5$, $F=1$, $\varepsilon=0.1$, $Pr=10$.

2 Secondary three-dimensional instability

We now study the secondary stability of two-dimensional permanent waves to infinitesimal three-di-

?1994-2018 China Academic Journal Electronic Publishing House. All rights reserved. http://www.cnki.net

mensional disturbances. The basic state $\bar{h}$ for the secondary instability is steady in a frame moving with the nonlinear phase speed c. Therefore, if we rewrite Eq. (3) using a coordinate transformation $x' = x - ct$, the resulting equation allows a solution of the form

$$h = \bar{h}(x') + \delta[H(x')e^{i(ly+\sigma t)} + c.c.], \quad (33)$$

where δ is the initial small amplitude, l is the spanwise wavenumber, and σ is the linear growth rate of the three-dimensional disturbance.

We substitute Eq. (33) into Eq. (3) and linearize in δ to obtain the following linear eigenvalue problem for $H(x')$ and σ:

$$\begin{aligned}
&\bar{h}^3 H^{\mathrm{IV}} + 3\bar{h}^2\bar{h}'H''' + \left(\frac{2G^2}{15S}\bar{h}^3 \right.\\
&+ \frac{5GMn}{12S}\left(Pr - \frac{8}{25}\right)\bar{h}^2 - \frac{1}{2}\frac{PrMn^2}{S}\bar{h} - 2l^2\Big)\bar{h}^3 H''\\
&+ \left(3\bar{h}^2\bar{h}''' + \frac{8G^2}{5S}\bar{h}^5\bar{h}' + \frac{25GMn}{6S}\left(Pr - \frac{8}{25}\right)\bar{h}^4\bar{h}'\right.\\
&- \frac{4PrMn^2}{S}\bar{h}^3\bar{h}' + \frac{G}{\varepsilon S}\bar{h}^2 - \frac{Mn}{\varepsilon S}\bar{h} - \frac{c}{\varepsilon S}\\
&\left. - 3l^2\bar{h}^2\bar{h}'\right)H' + \left[3(\bar{h}^2\bar{h}''')' + \frac{4G^2}{5S}(\bar{h}^5\bar{h}')'\right.\\
&+ \frac{25GMn}{12S}\left(Pr - \frac{8}{25}\right)(\bar{h}^4\bar{h}')'\\
&- \frac{2PrMn^2}{S}(\bar{h}^3\bar{h}') + \frac{2G}{\varepsilon S}\bar{h}\bar{h}' - \frac{Mn}{\varepsilon S}\bar{h}' + l^4\bar{h}^3\\
&\left. - \frac{PrMn}{2S}l^2\bar{h}^4\left(\frac{5}{6}G\bar{h} - Mn\right) + \frac{\sigma}{\varepsilon S}\right]H = 0, \quad (34)
\end{aligned}$$

where prime denotes differentiation and IV denotes fourth derivative with respect to x'. The coefficients in Eq. (34) are periodic in x', and the Floquet theorem allows us to express the solution of Eq. (34) as

$$H = e^{i\lambda kx'}\sum_{n=-N}^{N} c_n e^{iknx'}, \quad (35)$$

where $H(x')$ represented by the finite Fourier sum has the same period $2\pi/k$ as the coefficients of Eq. (34) and λ is the Floquet exponent. If $\lambda = 0$, the eigenfunction H has the same period as the base state $\bar{h}$, and we are led to study the synchronous solutions with wavelength $2\pi/k$, as performed by Orszag and Patera[15] for wall-bounded shear flows. If $\lambda = \pm\frac{1}{2}$, the principal subharmonic solutions can be studied, the same as Herbert's studies[16] on plane channel flow.

2.1 Secondary synchronous instability ($\lambda = 0$)

It is proved that H in Eq. (34) can be replaced by its complex conjugate H^*. So $H + H^*$ is also the solution of Eq. (34), which means the eigenfunction of Eq. (34) is real. Thus H is expressed as the real Fourier form for $\lambda = 0$:

$$\begin{aligned}
H = \frac{a_0}{2} &+ a_1\cos(kx') + b_1\sin(kx')\\
&+ a_2\cos(2kx') + b_2\sin(2kx'). \quad (36)
\end{aligned}$$

Substituting Eq. (36) into Eq. (34) and integrating it in a period domain $2\pi/k$ with weighted functions 1, $\cos(kx')$, $\sin(kx')$, $\cos(2kx')$, and $\sin(2kx')$, we can obtain a 5×5 real-eigenvalue matrix problem. The eigenvalues σ are then obtained from the resulting fifth-degree characteristic equation. The results are given in Figs. 7—11 with all kinds of parameters. For isothermal film, our results are the same as that of Joo and Divas[8].

In Fig. 7, when the temperature increases along the plate, the film flow of the secondary instability becomes more unstable, i.e. the growth rate σ and the cutoff spanwise wavenumber l_c increase. In Fig. 8, when the streamwise wavenumber reduces to $k = k_m$, the growth rate of the secondary instability becomes larger. In Fig. 9, the effect of Reynolds number is the same as the isothermal case: as the mean layer thickness (or G) increases, the growth rate and the cutoff spanwise wavenumber l_c increase.

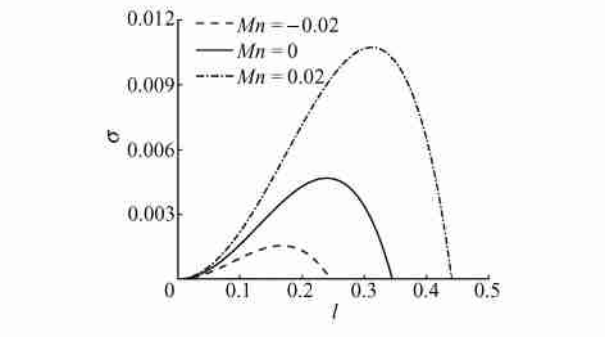

Fig. 7. Growth rates of the three-dimensional synchronous instability versus the spanwise wavenumber with different Marangoni numbers. $G = 5$, $F = 1$, $\varepsilon = 0.1$, $Pr = 10$, $k = k_m$.

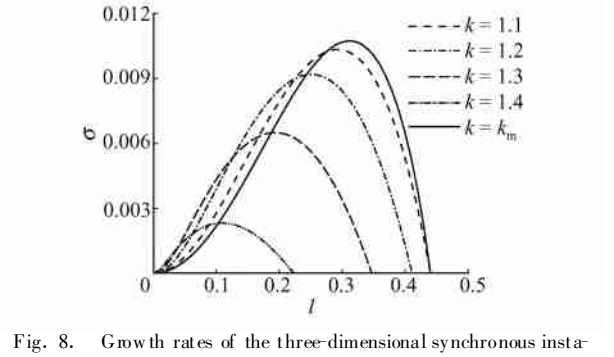

Fig. 8. Growth rates of the three-dimensional synchronous instability versus the spanwise wavenumber with different streamwise wavenumbers. $Mn = 0.02$, $G = 5$, $F = 1$, $\varepsilon = 0.1$, $Pr = 10$.

?1994-2018 China Academic Journal Electronic Publishing House. All rights reserved. http://www.cnki.net

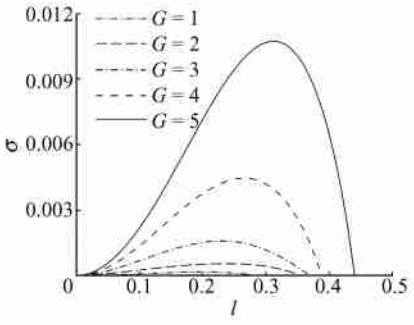

Fig. 9. Growth rates of the three-dimensional synchronous instability versus the spanwise wavenumber with different Reynolds numbers. $Mn=0.02$, $F=1$, $\varepsilon=0.1$, $Pr=10$, $k=k_m$.

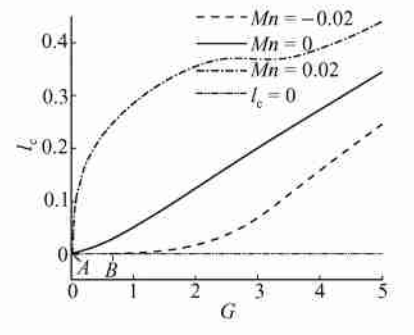

Fig. 10. Cutoff disturbance wavenumber l_c of the three-dimensional synchronous instability versus Reynolds number with different Marangoni numbers. $F=1$, $\varepsilon=0.1$, $Pr=10$, $k=k_m$.

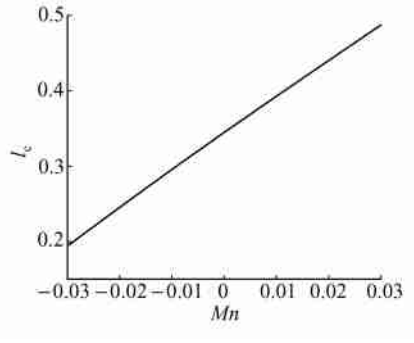

Fig. 11. Cutoff disturbance wavenumber l_c of the three-dimensional synchronous instability versus Marangoni number. $G=5$, $F=1$, $\varepsilon=0.1$, $Pr=10$, $k=k_m$.

In Fig. 10, when the Marangoni number is not zero, the critical value of G is not zero either, because there is not an unconditional instability of the two-dimensional waves now. Points A and B are the critical Reynolds number with the values of 0.023853 and 0.628853, corresponding to $Mn=0.02$ and $Mn=-0.02$, respectively, for both the primary instability and the secondary synchronous instability. The curve in Fig. 11 is exactly a line according to our computation, which also shows that the Marangoni number has destabilization effect on the secondary instability.

2.2 Secondary subharmonic instability $\left(\lambda=\pm\frac{1}{2}\right)$

Similar to the analysis of secondary synchronous instability above, H is expressed as real Fourier form for $\lambda=\pm\frac{1}{2}$:

$$H=a_1\cos(kx'/2)+b_1\sin(kx'/2)+a_2\cos(3kx'/2)+b_2\sin(3kx'/2). \quad (37)$$

Substituting Eq. (37) into Eq. (34) and integrating it in a period domain $4\pi/k$ with weighted functions $\cos kx'/2$, $\sin(kx'/2)$, $\cos(3kx'/2)$, and $\sin(3kx'/2)$, we can obtain a 4×4 real-eigenvalue matrix problem. The eigenvalues σ can also be obtained easily from the resulting fourth-degree characteristic equation. Figure 12 shows the growth rates of the three-dimensional subharmonic instability versus the spanwise wavenumber for different values of Marangoni number, streamwise wavenumber, and Reynolds number. We can see that there exist two modes of three-dimensional subharmonic instability: one is surface wave instability within the long wave domain, the other is thermocapillary instability within moderate wavenumber. The growth rates of the two modes both increase with the increasing of the Marangoni number. For surface wave instability, the increase of Reynolds number and the decrease of streamwise wavenumber make the growth rate increase, which is the same as the secondary synchronous instability. But for thermocapillary instability, the increase of Reynolds number and the decrease of streamwise wavenumber make the growth rate decrease, which shows that the increase of inertia weakens the thermocapillary instability.

3 Conclusion

In this paper, secondary instabilities of linearly heated falling films are studied by three steps. First the analysis of the primary linear instability on the undisturbed surface is performed; then the similar Landau equation is obtained through nonlinear saturation of primary instability into two-dimensional finite-amplitude permanent wave; the secondary (three-dimensional) instability of the two-dimensional wave is studied by the Floquet theorem. This paper identifies the existence of secondary synchronous instability and secondary subharmonic instability, and also investigates their growth rates with the spanwise wavenumber for different values of Marangoni number, streamwise wavenumber and Reynolds number.

?1994-2018 China Academic Journal Electronic Publishing House. All rights reserved. http://www.cnki.net

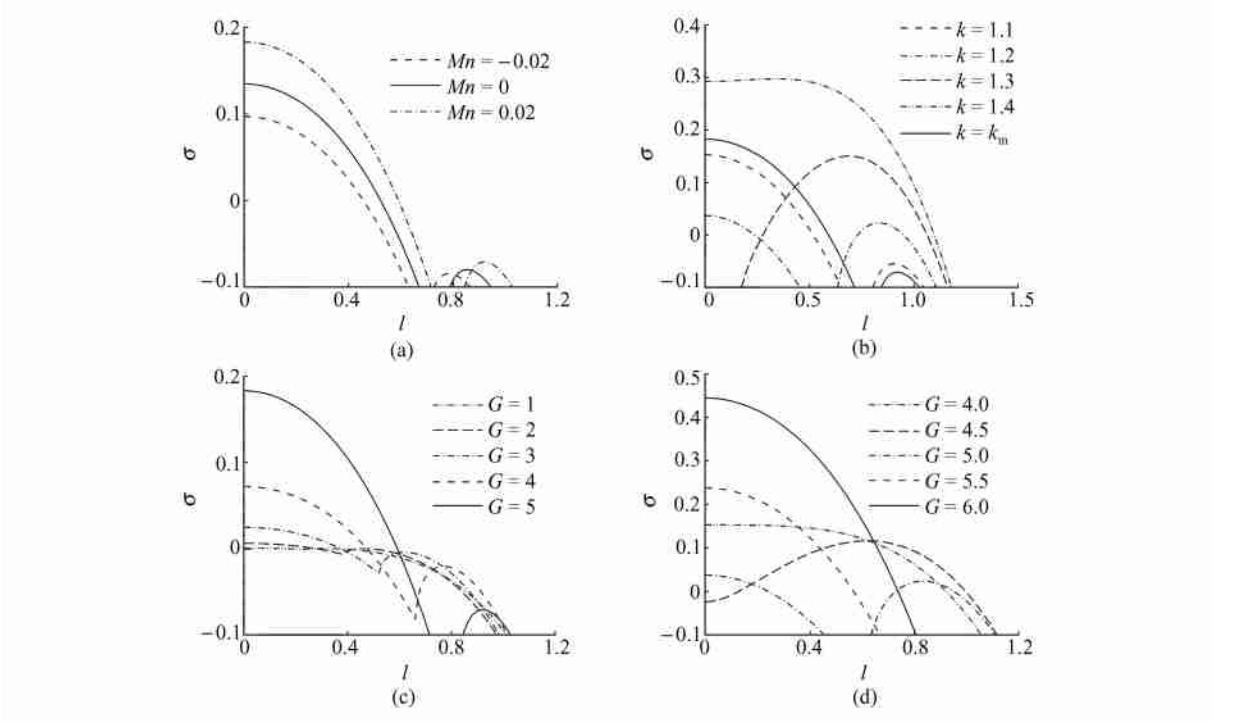

Fig. 12. Growth rates of the three-dimensional subharmonic instability versus the spanwise wavenumber for different values of Marangoni number, streamwise wavenumber and Reynolds number for $F=1$, $\varepsilon=0.1$, $Pr=10$. (a) $G=5$, $k=k_m$; (b) $G=5$, $Mn=0.02$; (c) $Mn=0.02$, $k=k_m$; (d) $Mn=0.02$, $k=1.2$.

Appendix: Coefficients of Eqs. (16) and (17)

$$\alpha_1=-\mathrm{i}k(G-Mn)+k^2\varepsilon\left[\frac{2}{15}G^2-\frac{2}{15}GMn\left(1-\frac{25}{8}Pr\right)-\frac{1}{2}PrMn^2-k^2S\right],$$

$$\beta_1=-\mathrm{i}k(2G-Mn)+k^2\varepsilon\left[\frac{4}{5}G^2-\frac{2}{3}GMn\left(1-\frac{25}{8}Pr\right)-2PrMn^2-21k^2S\right],$$

$$\gamma_1=-\mathrm{i}kG+k^2\varepsilon\left[2G^2-\frac{4}{3}GMn\left(1-\frac{25}{8}Pr\right)-3PrMn^2-3k^2S\right],$$

$$\alpha_2=-2\mathrm{i}k(G-Mn)+k^2\varepsilon\left[\frac{8}{15}G^2-\frac{8}{15}GMn\left(1-\frac{25}{8}Pr\right)-2PrMn^2-16k^2S\right],$$

$$\beta_2=-\mathrm{i}k(2G-Mn)+k^2\varepsilon\left[\frac{8}{5}G^2-\frac{4}{3}GMn\left(1-\frac{25}{8}Pr\right)-4PrMn^2-6k^2S\right],$$

$$\gamma_2=-2\mathrm{i}kG+k^2\varepsilon\left[8G^2-\frac{16}{3}GMn\left(1-\frac{25}{8}Pr\right)-12PrMn^2-48k^2S\right].$$

References

1 Kapitza P. L. Wave flow of thin viscous fluid layers. Zh. Eksp. Teor. Fiz., 1948, 18: 3—28; also in: Collected Works of P. L. Kapitza. Oxford: Pergamon, 1965.

2 Kapitza P. L. and Kapitza S. P. Wave flow of thin fluid layers of liquid. Zh. Eksp. Teor. Fiz., 1949, 19: 105—120; also in: Collected Works of P. L. Kapitza. Oxford: Pergamon, 1965.

3 Chang H. C. Wave evolution on a falling film. Annu. Rev. Fluid Mech., 1994, 26: 103—136.

4 Oron A., Davis S. H. and Bankoff S. G. Long-scale evolution of thin liquid films. Rev. Mod. Phys., 1997, 69: 931—980.

5 Kalitzova-Kurteva P., Slavtchev S. and Kurtev I. Linear instability in liquid layers on an inclined, non-uniformly heated wall. J. Theor. Appl. Mech., 2000, 30(4): 12—23.

6 Miladinova S., Slavtchev S., Lebon G. et al. Long-wave instabilities of non-uniformly heated falling films. J. Fluid Mech., 2002, 453: 153—175.

7 Benney D. J. Long waves on liquid films. J. Maths. Phys., 1966, 45: 150—155.

8 Joo S. W. and Davis S. H. Instabilities of three-dimensional viscous falling films. J. Fluid Mech., 1992, 242: 529—547.

9 Roskes G. J. Three-dimensional long waves on a liquid film. Phys. Fluids, 1970, 13: 1440—1445.

10 Gjevik B. Occurrence of finite-amplitude surface waves on falling liquid films. Phys. Fluids, 1970, 13: 1918—1925.

11 Lin S. P. Finite amplitude side-band stability of a viscous film. J. Fluid Mech., 1974, 74: 417—429.

12 Chang H. C. Onset of nonlinear waves on falling films. Phys. Fluids, 1989, A(1): 1314—1327.

13 Joo S. W., Davis S. H. and Bankoff S. G. Long-wave instabilities of heated falling films: two-dimensional theory of uniform layers. J. Fluid Mech., 1991, 230: 117—146.

14 Boyd J. P. Chebyshev and Fourier Spectral Methods. 2nd ed. New York: Dover Publications Inc., 1999.

15 Orszag S. A. and Patera A. T. Secondary instability of wall-bounded shear flows. J. Fluid Mech., 1983, 128: 347—385.

16 Herbert T. Secondary instability of plane channel flow to subharmonic three-dimensional disturbance. Phys. Fluids, 1983, 26: 871—874.

?1994-2018 China Academic Journal Electronic Publishing House. All rights reserved. http://www.cnki.net